NASA Technical Memorandum 100759

Analysis of Altimetry Over the Aral Sea

Andrew Y. Au, Richard D. Brown,
and Jean E. Welker

April 1991

NASA

NASA Technical Memorandum 100759

Analysis of Altimetry Over the Aral Sea

Andrew Y. Au and Richard D. Brown
ST Systems Corporation
Lanham, Maryland

Jean E. Welker
NASA-Goddard Space Flight Center
Greenbelt, Maryland

National Aeronautics and
Space Administration

Goddard Space Flight Center
Greenbelt, MD

1991

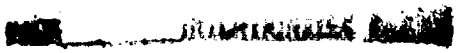

PREFACE

Satellite-based altimetric data taken by GEOS-3, SEASAT and GEOSAT over the Aral Sea are analyzed and a least-squares collocation technique is used to predict the geoid undulations on a 0.25° x 0.25° grid and to transform these geoid undulations to free air gravity anomalies. Rapp's 180 x 180 geopotential model is taken as the reference model. The collocation procedure is performed with a set of local residual empirical covariance functions. For comparison, Rapp's global covariance functions and Jordan's self-consistent theoretical covariance functions based on Jordan's formulation and on locally derived parameters are also used to grid geoid undulations and to predict gravity anomalies. The sensitivity of the collocation results to the choice of covariance functions is discussed.

CONTENTS

LIST OF FIGURES

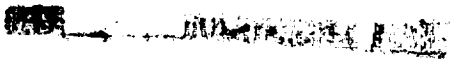

INTRODUCTION

This project involved the processing of satellite altimeter data over the Aral Sea in Soviet Central Asia for the recovery of area-mean gravity information. Gravity information in this area of the world is not readily available, so the possibility of obtaining it from the processing of altimeter observations is attractive. The mean surface level of the seas approximates an equipotential surface. Therefore, information about the underlying gravity potential and its derivative, gravity, can be obtained by measuring the relative shape of this surface by means of altimetry.

Local gravity anomalies recovered from satellite-based altimeter data have been performed by Knudsen (1987, 1988) in 2° x 2° areas in the North Atlantic Ocean, by Mazzega and Houry (1989) in the Mediterranean and Black Seas, and by Au *et al.* (1989a) over the Black and Caspian Seas. The local covariance functions used in the works of Knudsen (1987, 1988) and Mazzega and Houry (1989) are determined from spectral analysis of global models, whereas those in our previous work are determined by numerical convolution. Although these two processes are ideally equivalent given complete global data, the convolution method ensures the integration of available local information into the covariance functions.

Our principal objective for this project was to extend our previous analysis over the Aral Sea. The basic approach to the project can be divided into five steps:

1. Edit the geoid height data to remove any overland data.
2. Evaluate the geoid height differences at crossover points.
3. Remove the orbit errors from geoid heights using crossover differences.
4. Grid the geoid height data at 0.25° x 0.25° intervals.
5. Estimate 0.25° x 0.25° gravity anomalies from the gridded geoid heights using the collocation technique.

Step 1 is needed to ensure that only relevant data are included in the analysis. Steps 2 and 3 are necessary because satellite altimeter measurements cannot yield accurate sea-surface heights unless differences in satellite heights (orbit differences) from pass to pass are rectified and reduced to a common reference. If the mean sea-surface height at a given location is constant over the time span of the altimeter data used, any difference in surface height between two altimeter passes at the point where they cross is attributable primarily to orbit differences (although differences up to about 50 cm could be a consequence of tides--especially solid earth tides--whose amplitudes are about 25 cm).

Since orbit differences and earth tides are essentially constant for the short arcs over the Aral Sea, removal of a constant bias from all the crossover differences of a given pass should effectively remove all such errors. Area-mean surface height values are determined and reduced to the reference geoid in step 4. In step 5, these area-mean geoid heights are processed and area-mean gravity anomaly values are predicted using a linear least-squares estimation technique, called collocation, formulated by Moritz (1978). As applied herein, the collocation technique is essentially a differential operation transforming geopotential information to its first derivative--gravity.

Knowledge of the statistical correlation between area-mean geoid heights and gravity anomalies is required in the geoid-to-gravity transformation.

Of the three sources of altimeter data used, GEOS-3 altimeter data is of lesser quality (standard deviation between 25 and 50 cm, depending on operating mode) than that of SEASAT (6 to 10 cm, primarily because SEASAT used an advanced radar altimeter design), which is, in turn of lesser quality than GEOSAT (5 cm). The two GEOS-3 altimeter operating modes, intensive and global, are differentiated primarily by data rate, which explains the corresponding difference in quality. The GEOS-3 mission collected data between 1975 and 1978 over latitudes up to 65 degrees, whereas SEASAT collected data only during 100 days in 1978 over latitudes up to 72 degrees. GEOSAT, in orbit since October 1986, repeated the same ground track as the ill-fated SEASAT in a 17-day Exact Repeat Mission (ERM).

The preliminary clean-up processes applied to the altimetry data are discussed in the next section. Results of the application of least-squares collocation to both geoid gridding and gravity prediction are presented in section III. The results are then discussed in section IV. Prototype computer programs used in both data processing and collocation can be found in Au *et al.* (1989b).

II. ALTIMETER DATA

The altimeter data over the Aral Sea, obtained from NASA/GSFC via the Geodynamics Group of ST Systems Corporation (STX), were processed with the GEODYN Tracking Data Formatter and was written in GEODYN format. There are seven GEOS-3 passes, 16 SEASAT passes, and 151 GEOSAT passes comprising 3069 data records over the Aral Sea. The geodetic positions of these satellite passes over the Aral Sea and typical ground-track profiles of these passes are shown in Figures 1 and 2, respectively.

It can be inferred from Figure 1 that the data coverage is inhomogeneous and incomplete. There are data gaps in the northwestern and southeastern regions of the sea. The quality of the data observed in Figure 2 is also disappointing. There is a large number of data spikes, especially at the beginning and end of each ground-track profile. Because it is difficult to distinguish the signal from the noise in an unadjusted satellite pass, over-enthusiastic data cleaning will result in unnecessary sacrifice in the already-small data set. Data spikes were, therefore, not edited out prior to our crossover adjustment to the satellite pass. After this adjustment, questionable data records were examined to determine if they resulted from a loss-of-phase lock, particularly if they occurred at the beginning or end of a pass. Noisy data records were then removed from subsequent analysis.

Crossover Adjustments

The major error source in altimetric geoid undulations is the uncertainty in determining the radial component of the satellite trajectory. This uncertainty is manifest in the misclosure of surface elevation at the intersections of ground tracks (crossovers) of different passes. For the short arcs of data considered here, the orbit error can be modeled as a bias applied to all the data of a given pass. These pass biases are adjusted such that crossover differences are minimized, holding one pass fixed so that all the satellite passes can be defined with respect to a common reference model. A detailed description of the crossover adjustment process can be found in Au *et al.* (1989a).

The standard errors assumed in the weighted least-squares crossover adjustments are 25 cm for GEOS-3, 10 cm for SEASAT, and 5 cm for GEOSAT. The pass having the maximum number of crossovers was chosen as the reference pass. The bias for the reference pass was not solved for, but the reference pass was adjusted with the other passes following the crossover adjustment process to achieve a best fit to the average geoid height of the reference geopotential model. Rapp's 180 x 180 model is the reference geopotential model used in this study. An error covariance matrix of the crossover adjustment was also determined. This error covariance matrix adds a crossover adjustment error to the error associated with each satellite pass.

From the geometry of altimeter passes in the current data set, there are at most, 3221 crossovers over the Aral Sea. These possible crossover locations were carefully checked and eliminated if they occurred at data gaps, which are defined to be part of a satellite arc that did not have an altimeter observation within 70 km (about 10 seconds in time).

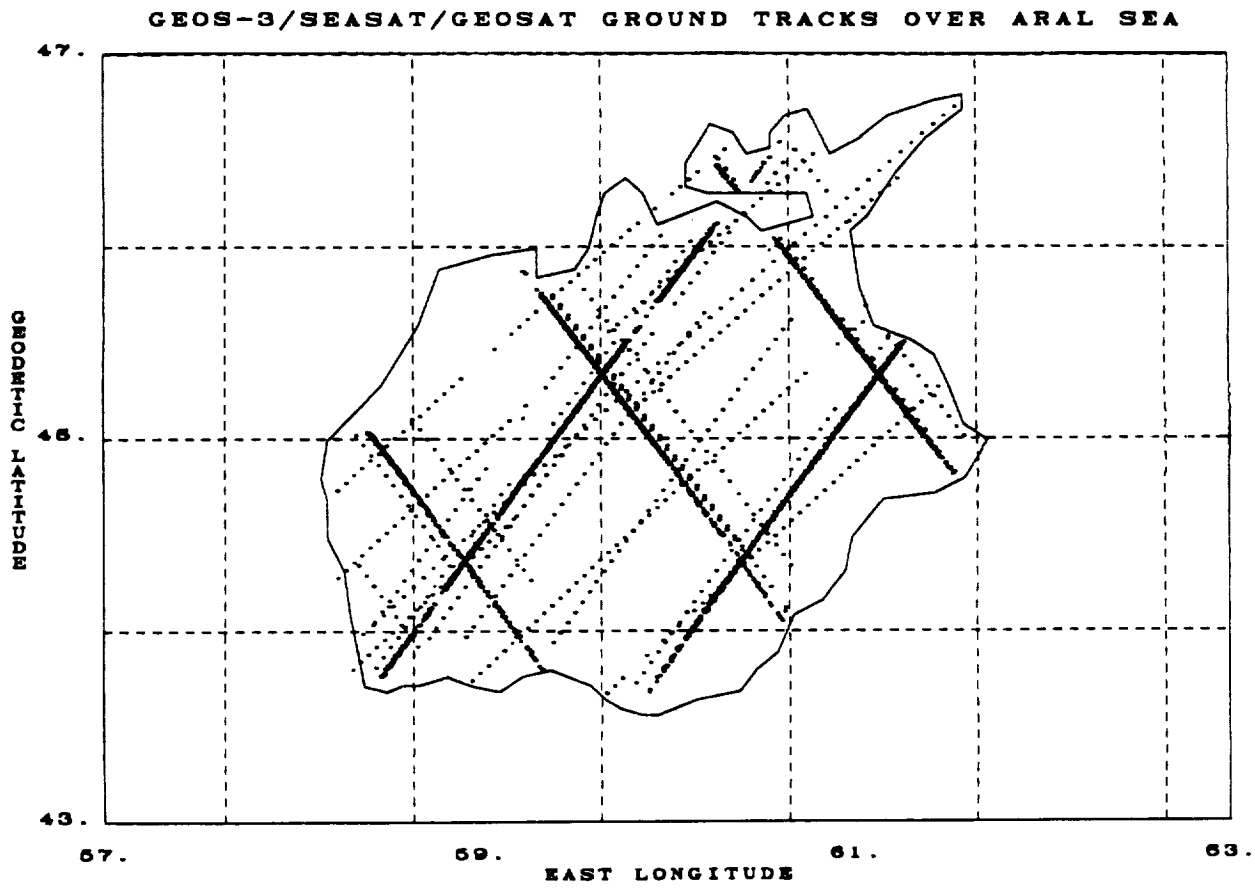

Figure 1. GEOS-3, SEASAT and GEOSAT altimeter data distribution over the Aral Sea.

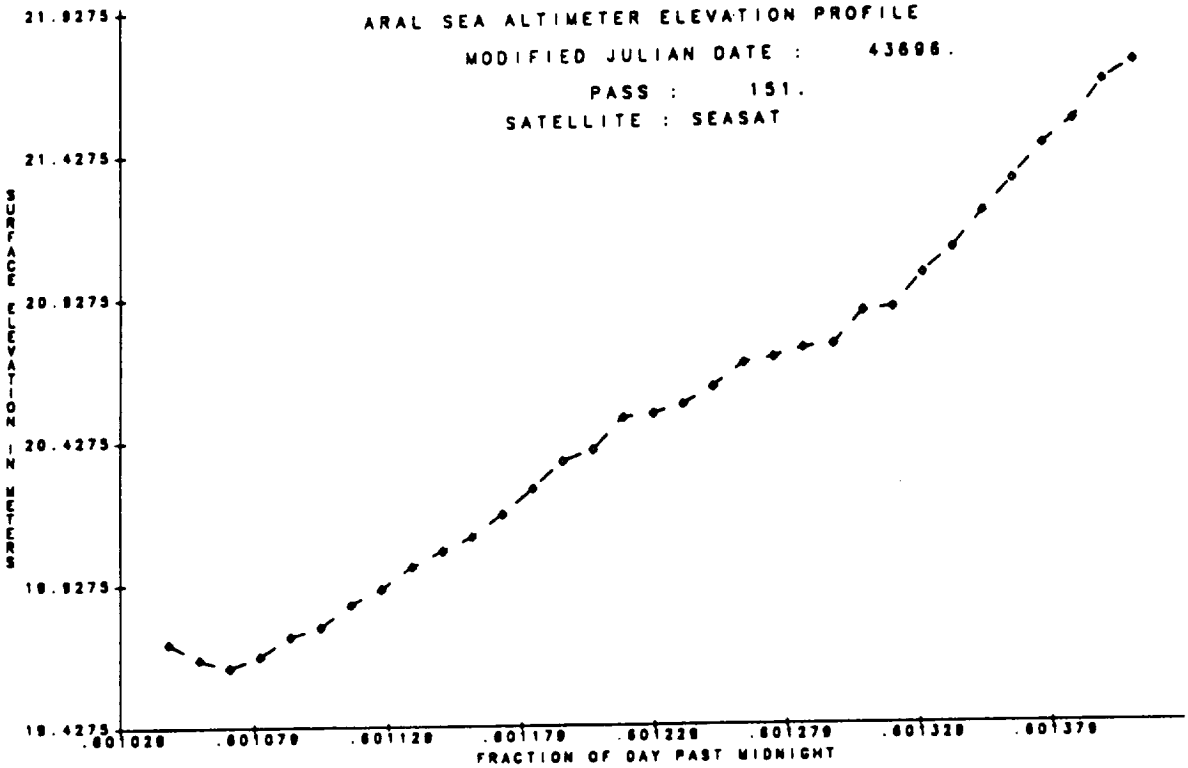

Figure 2a. Sample altimeter elevation profile of the Aral Sea--relatively noiseless profile.

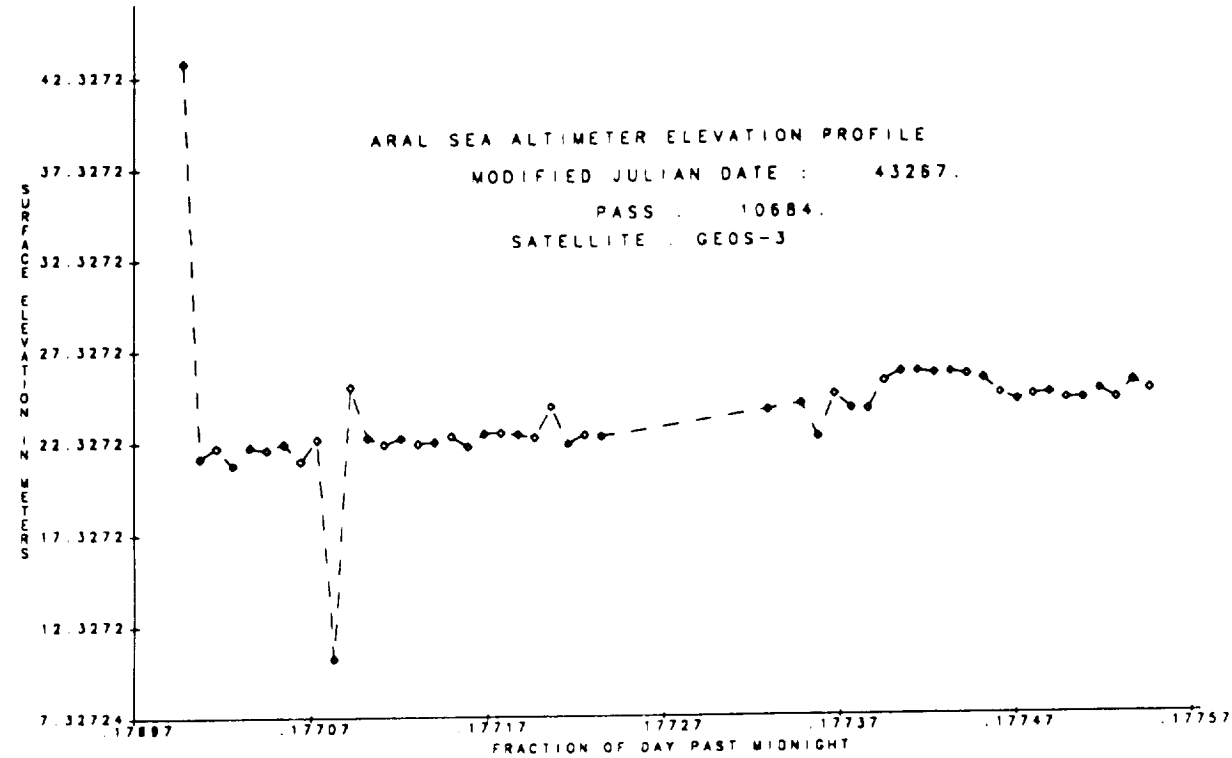

Figure 2b. Sample altimeter elevation profile of the Aral Sea--profile with a data spike.

Such editing reduced the number of crossovers to 1136--none of which is GEOS-3 with GEOS-3. Thirty are SEASAT with SEASAT, 803 are GEOSAT with GEOSAT, 17 are GEOS-3 with SEASAT, 85 are GEOS-3 with GEOSAT, and 201 are SEASAT with GEOSAT. The RMS (root mean square) of the crossover residuals before the crossover adjustment is 5.70 m. The RMS after crossover adjustment is reduced to 17 cm. The reference pass is GEOS-3 pass #6547. The adjusted profile of this reference pass and its corresponding reference geoid model are shown in Figure 3.

Preliminary Analysis of the Adjusted Data

The adjusted data must be gridded for geodetic collocation analyses. This is a time-consuming process unless the data records are properly arranged. A sort/merge process (Au *et al.*, 1989a) was used to group data records for a chosen cap size of a quarter degree.

For an initial assessment of the quality of the altimeter data, geoid undulations were gridded according to the method of weighted averages. The weight of a data point with respect to a grid point is a function of the square of its distance from the grid point. A contour map of the weighted-average geoid undulations is shown in Figure 4. The contour map of these geoid undulations according to the reference geopotential model, Rapp's 180 x 180 model, is shown in Figure 5. The contour map of the gridded weighted-average geoid resembles that of the reference geoid of the Aral Sea. In spite of the limited data coverage in the gridded geoid, it is seen that there is considerably more short-wavelength information content in the altimeter data over the Aral Sea than in the reference geoid.

III. APPLICATION OF COLLOCATION TECHNIQUE

Collocation is a predictive method based on linear least-squares interpolation, in which a stochastic spatially averaged correlation between observables in the data space is assumed. The auto-correlation function, which reflects a spatial correlation of observables in a data space, is used for interpolation. For transformations from a data space into a prediction space, a cross-correlation function, which represents the spatial correlation between variables in the data space and the prediction space, is required. In least-squares collocation, these corrrelation functions are the geoid-geoid, geoid-gravity and gravity-gravity covariance functions.

Collocation Gridding of Geoid Undulations

According to the linear least-squares interpolation formula (Au *et al.*, 1989a), the predicted geoid undulation $N(P)$ at a point P is given by

$$N(P) = C_{PN}(C_{NN}+D)^{-1}N_P \qquad (1)$$

where C_{PN} is a covariance vector relating the undulation at P to the observable in the neighborhood of P, C_{NN} is the stochastic covariance matrix, D is the error covariance matrix that represents the random error associated with each observable and the error from crossover adjustments), and N_p is a column vector of geoid observables in the neighborhood of P.

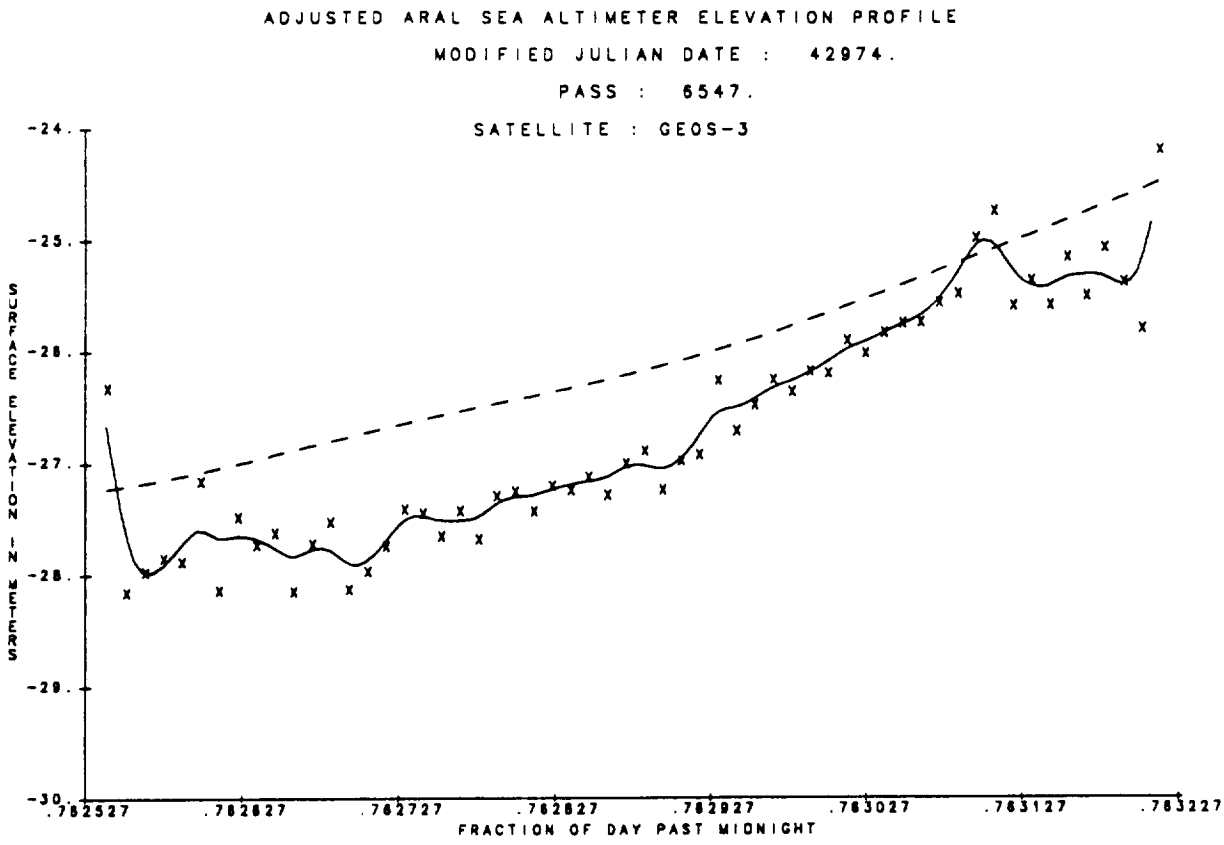

Figure 3. Sample adjusted altimeter elevation profile of the Aral Sea--profile of the reference pass. Dashed line is the Rapp's 180 x 180 reference geoid.

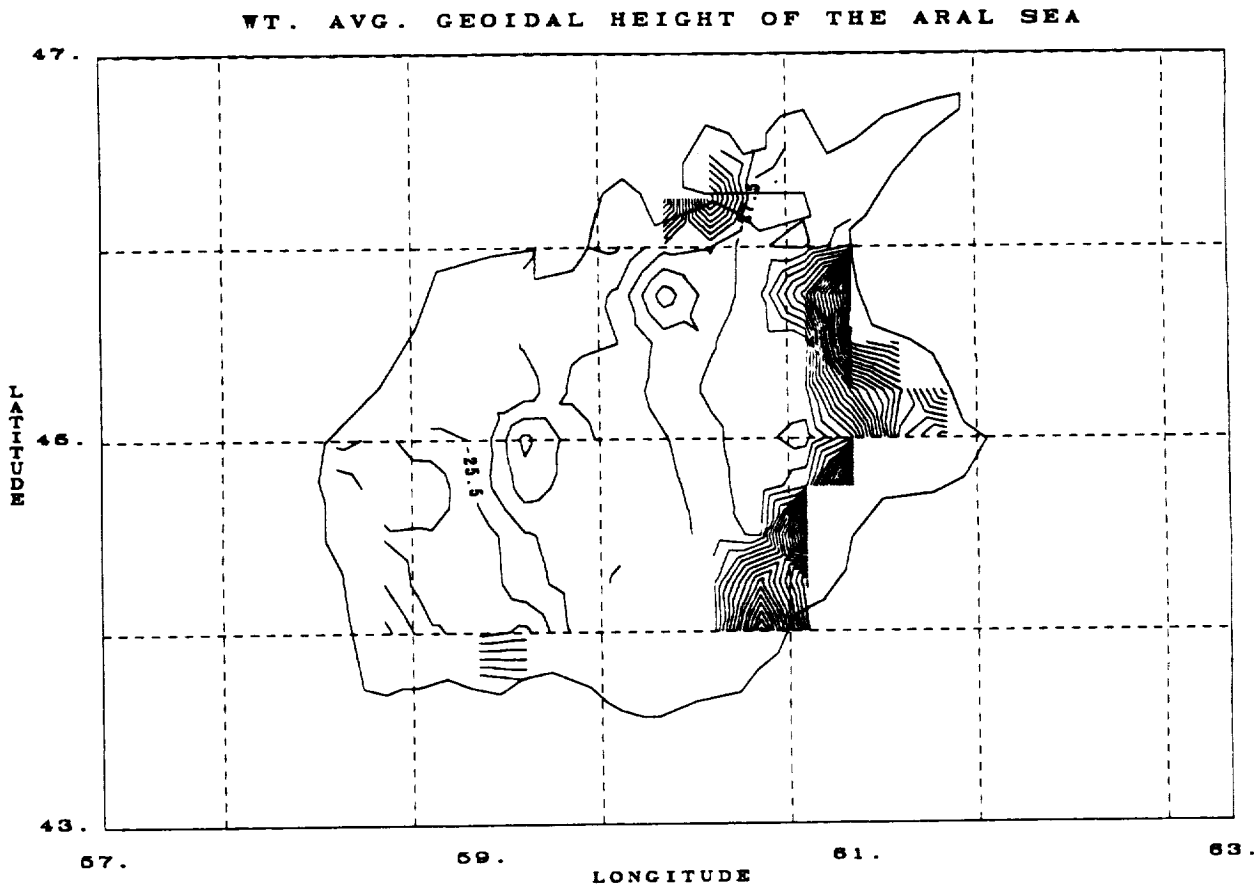

Figure 4. A contour map of the weighted-average geoid undulations (m above mean sea level) of the Aral Sea.

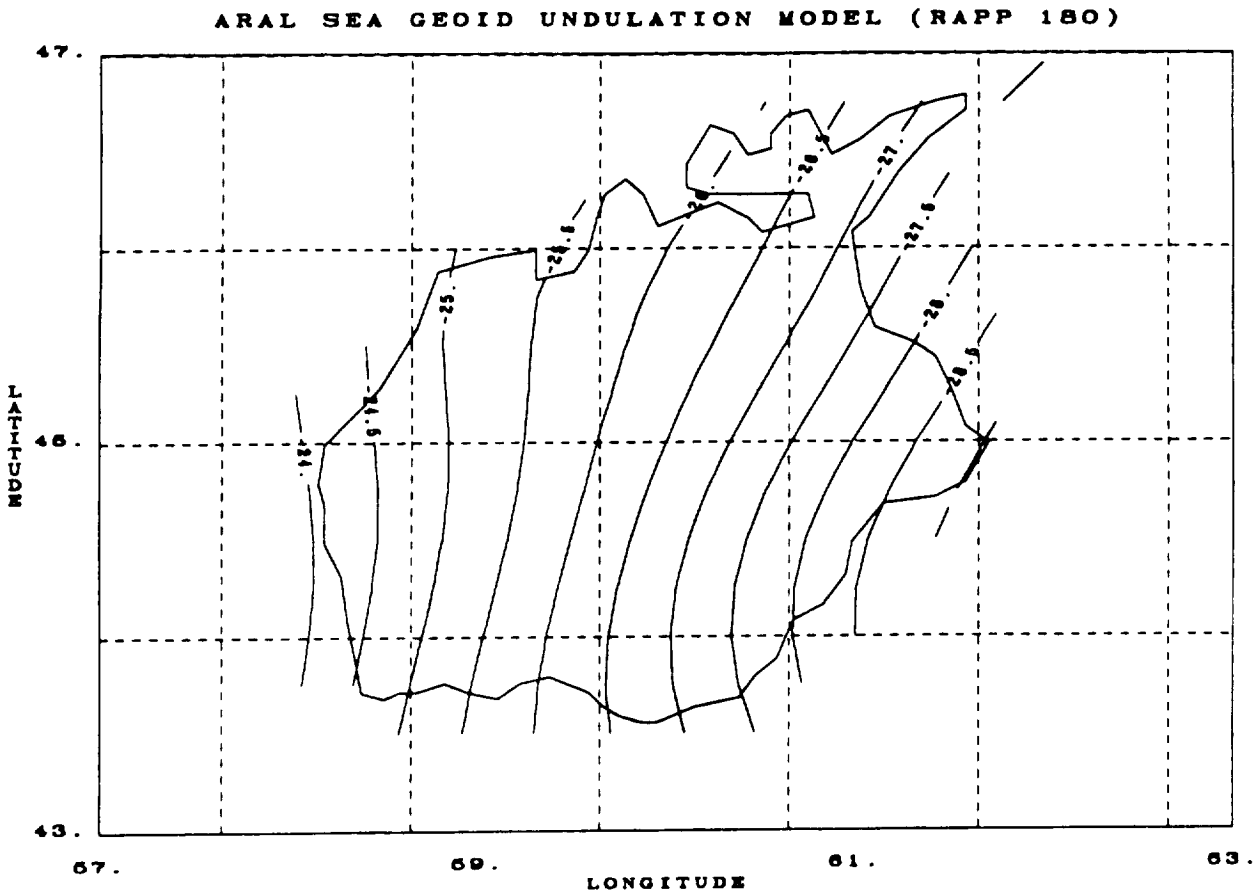

Figure 5. A contour map of Rapp's 180 x 180 reference geoid undulations (m above mean sea level) of the Aral Sea.

The stochastic covariance matrix is derived from a geoid-geoid auto-correlation function that reflects the averaged roughness and topographic correlation of the region concerned. In essence, an observable is assigned a weight in the interpolation process via the stochastic covariance matrix. For example, if the weights are assigned as a function of the inverse of the square of distance from the point at which prediction is made, the weighted-average results coincide with the collocation results. The variance at each gridded point is given by

$$\sigma^2 = C_o - C_{PN}(C_{NN})^{-1}C_{PN} \qquad (2)$$

where C_o is the square of the geoid-geoid covariance amplitude.

A variety of covariance functions are used in the literature. Common covariance functions are the global covariance functions based on Rapp's 180 x 180 global reference geopotential model (Rapp, 1986), the self-consistent covariance functions based on Jordan (Jordan, 1972) and local covariance functions derived for a specified region (Knudsen, 1987, 1988; Au *et al.*, 1989a). The effects of a particular choice of covariance functions on both geoid interpolation and geoid-to-gravity transformation for a local area such as the Black Sea and the Caspian Sea are discussed in Au *et al.* (1989a). A local covariance function seems to be a logical choice for the Aral Sea. In the current report, all three types of covariance functions will be used for geoid gridding.

A local empirical covariance function can be determined based on the difference between gridded weighted-average geoid undulations and the reference geoid derived from Rapp's 180 x 180 reference geopotential model. A technique described by Moritz (1978) is used to determine this local covariance function, which is constructed by the convolution of the difference between the weighted-average geoid data and the reference geoid. The resultant covariance function is, in effect, a least-squares filter (Treitel and Robinson, 1966), which determines the contribution of each observable to the predicted value at a grid point. A plot of the local empirical geoid-geoid covariance function is shown in Figure 6. A contour map of the geoid undulations of the Aral Sea gridded with this local empirical covariance function is shown in Figure 7. The estimated error (square root of the variance) of the interpolated geoid is about 40 cm. The gridded geoid resembles the reference geoid except for the enrichment of high-frequency information and steep gradients at the eastern and southern parts of the sea.

For comparison, hybrid local Jordan self-consistent covariance functions are also used for geoid gridding. The geoid-geoid covariance amplitude C_o and a correlation length L used to calculate the Jordan covariance functions are extracted from the empirical local covariance functions (shown in Figure 6). A plot of this geoid-geoid Jordan covariance function is shown in Figure 8. A contour map of the geoid undulations of the Aral Sea gridded with this hybrid covariance function is shown in Figure 9. The estimated error of this interpolated geoid is about 40 cm. It should be noted that the interpolation results are rather insensitive to the choice of covariance functions as long as reasonable effective weights are assigned to each observable (Au *et al.*, 1989a). Rapp's global geoid-geoid covariance function (shown in Figure 10) is also used to grid the geoid undulations of the Aral Sea, and the resultant contour map is shown in Figure 11. The estimated error in this geoid interpolation is about 10 cm. It should also be noted that the estimated errors in the collocation interpolation are directly proportional to the covariance amplitudes of the

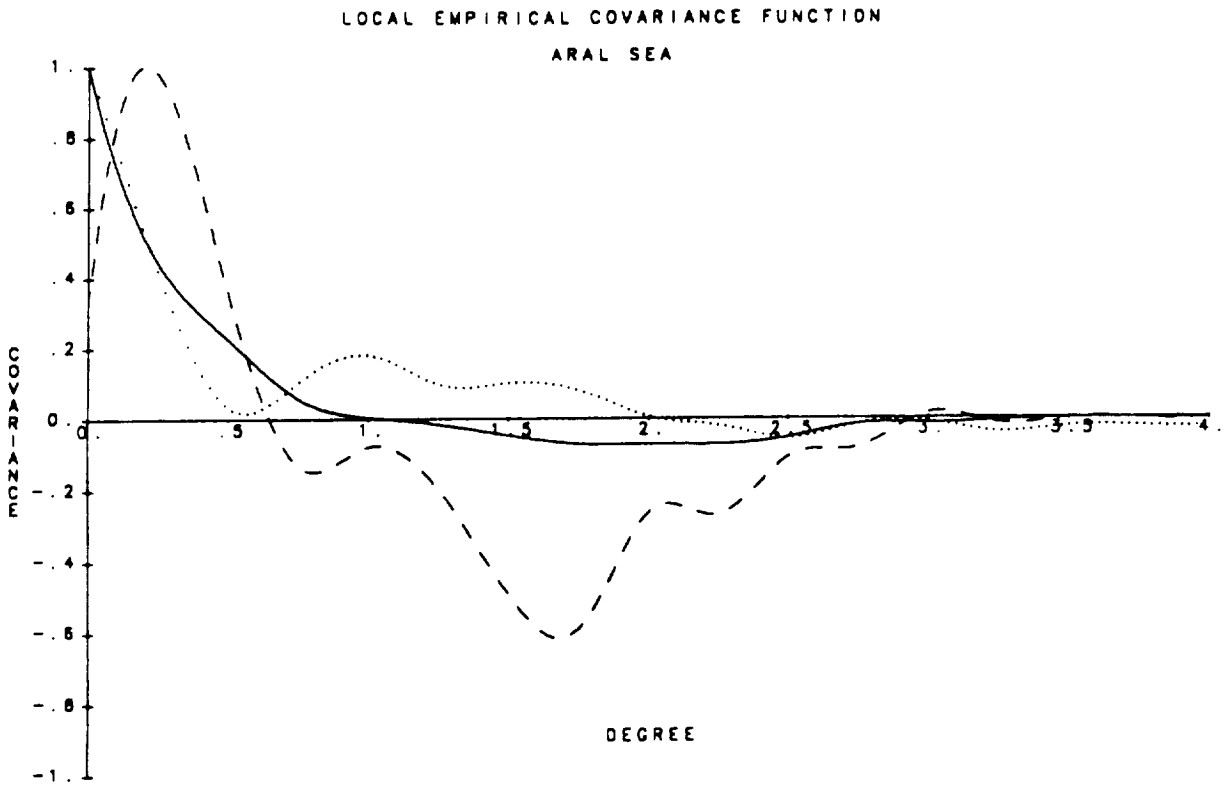

Figure 6. Normalized local residual empirical covariance functions of the Aral Sea. The normalized coefficients are:

1) 2.62 m^2 for geoid-geoid (solid line);
2) 11.14 m-mgal for geoid-gravity (dashed line), and
3) 1414 $(mgal)^2$ for gravity-gravity (dotted line).

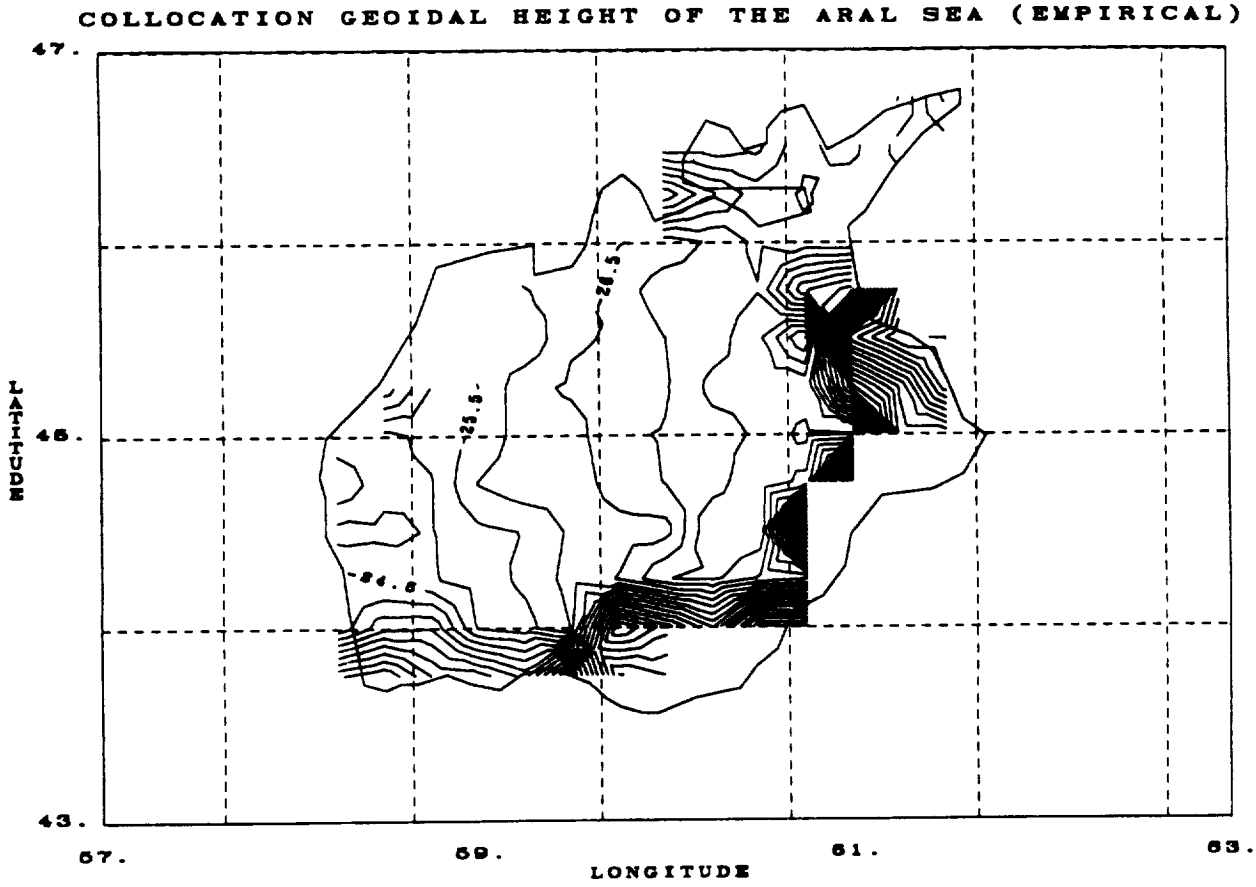

Figure 7. A contour map of the collocation geoid undulations (m above mean sea level) gridded with the local empirical geoid-geoid covariance function.

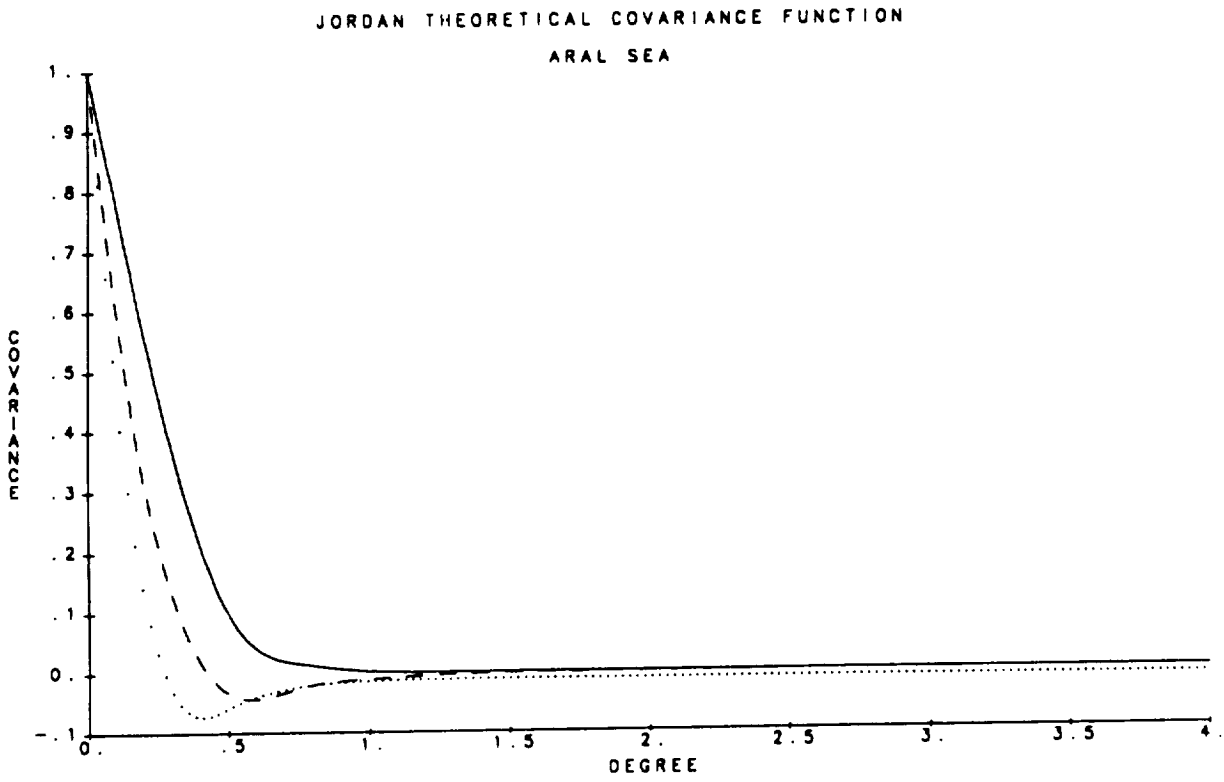

Figure 8. Normalized Jordan's theoretical covariance functions of the Aral Sea. The normalized coefficients are:

1) 2.62 m^2 for geoid-geoid (solid line);
2) 49.73 m-mgal for geoid-gravity (dashed line), and
3) 1414 $(mgal)^2$ for gravity-gravity (dotted line).

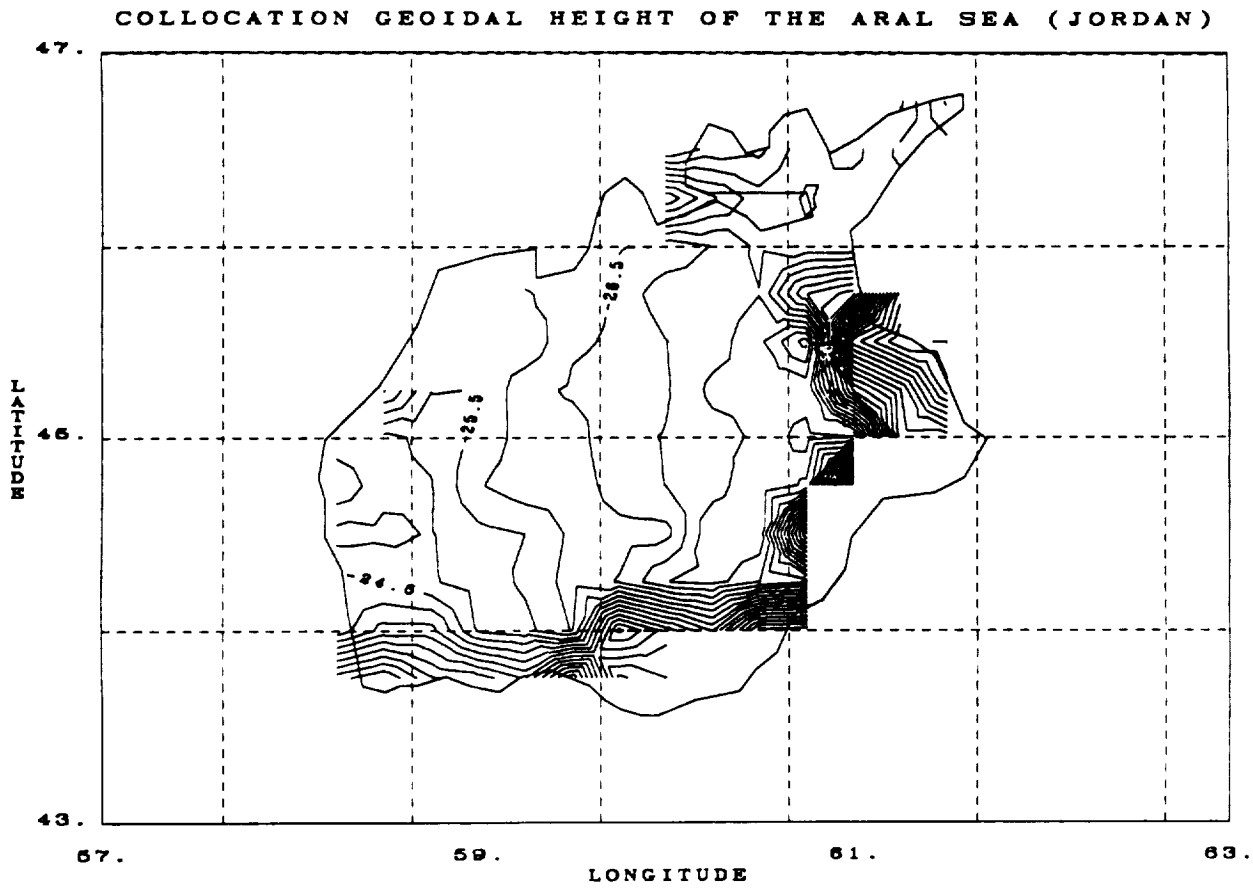

Figure 9. A contour map of the collocation geoid undulations (m above mean sea level) of the Aral Sea gridded with Jordan's geoid-geoid covariance function.

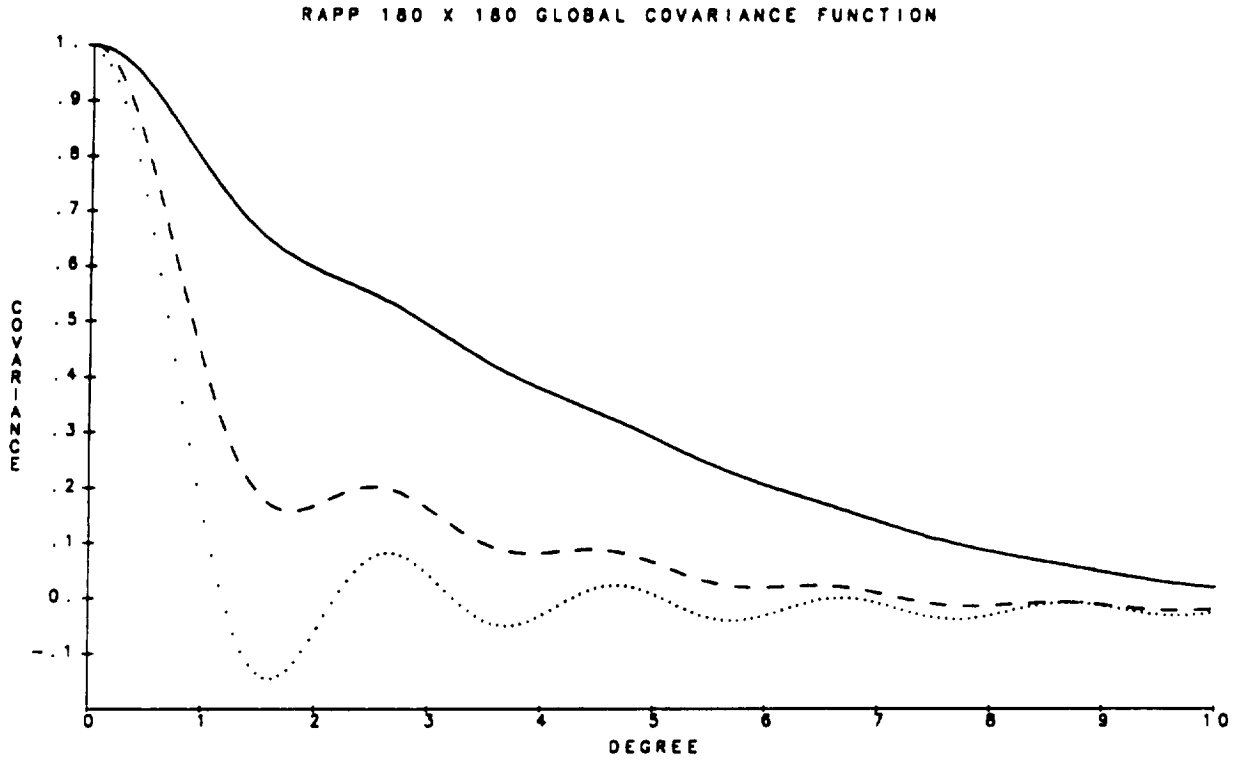

Figure 10. Normalized Rapp's 180 x 180 global covariance functions. The normalization coefficients are:

1) 1.13 m^2 for geoid-geoid (solid line);
2) 7.26 m-mgal for geoid-gravity (dashed line), and
3) 98.36 $(mgal)^2$ for gravity-gravity (dotted line).

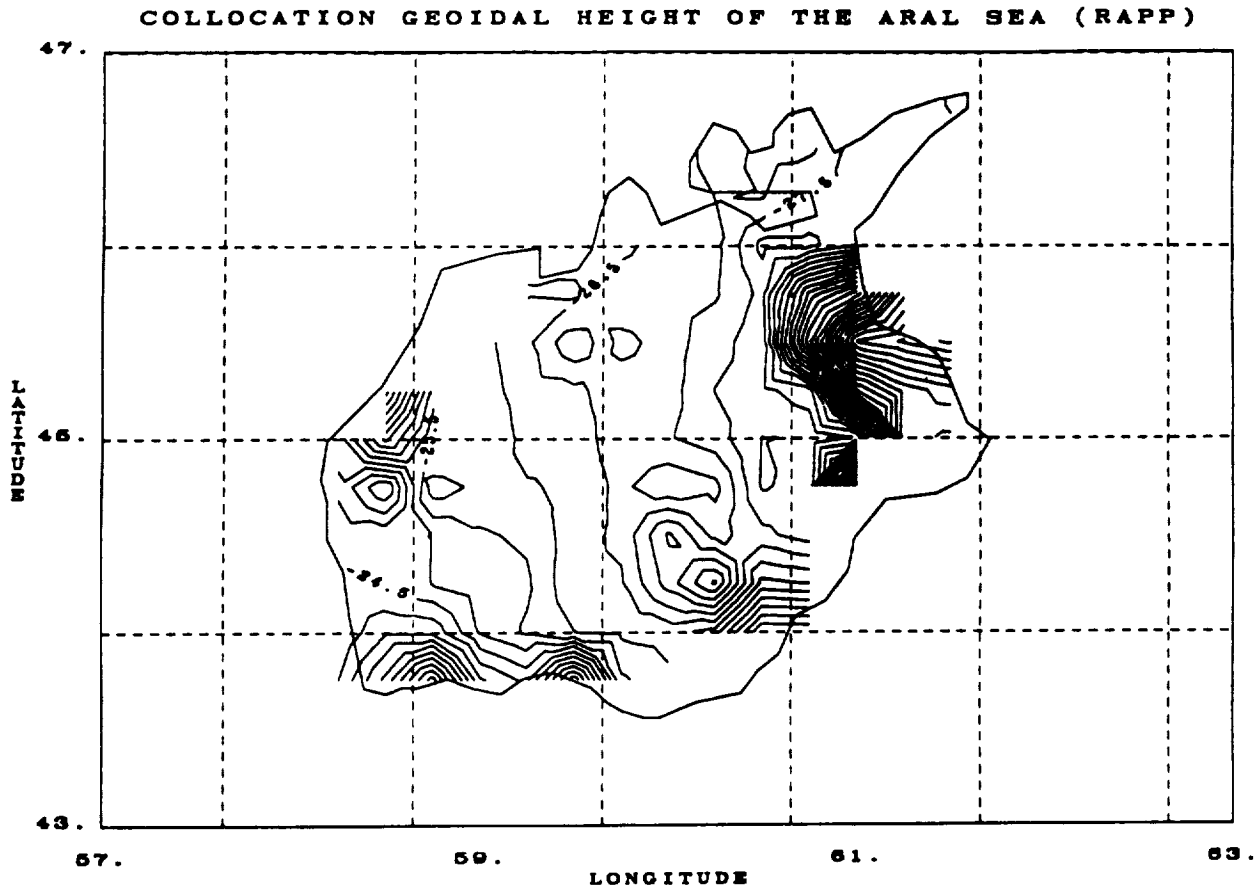

Figure 11. A contour map of the collocation geoid undulations (m above mean sea level) gridded with Rapp's global geoid-geoid covariance function.

covariance functions. The covariance amplitude of the local empirical geoid-geoid covariance is larger than that of the global geoid-geoid covariance function. The Aral Sea geoid is topographically rougher than the global average. A more realistic estimated error for the Aral Sea geoid interpolation is 40 cm.

Estimation of Gravity Anomalies

The geoid undulations can be transformed into gravity anomalies (Rapp, 1986) according to the equation

$$\Delta g = C_{gN}(C_{NN}+D)^{-1}(N-N_R) + \Delta g_R \qquad (3)$$

where Δg is the predicted point gravity anomaly, C_{gN} is the covariance vector of geoid-to-gravity transformation, C_{NN} is the covariance matrix for geoid-geoid interpolation, D is the error covariance matrix that is constructed from the variance of the previous interpolation of geoid undulations, N is the vector of gridded geoid undulations, N_R is the vector reference model's geoid undulations that correspond to each observed value of N, and Δg_R is the reference model's gravity anomaly value at the predicted grid point. The first term in equation (3) can be regarded as a perturbation on the reference gravity anomalies by the deviation of the observed geoid from the reference geoid. The variance is given by

$$\sigma^2 = C_{gg} - C_{gN}(C_{NN}+D)^{-1}C_{gN} \qquad (4)$$

where C_{gg} is the square of the gravity-gravity covariance amplitude. The input data for the geoid-to-gravity transformation include the geoid undulations gridded by collocation technique and the corresponding variances. Because a gridded data set contains far fewer data points than an ungridded data set, the strain on computer resources is greatly reduced by the choice of a gridded data set.

In order to perform the local geoid-to-gravity transformation, the local geoid-to-gravity covariance function must first be obtained. It is, however, the information we are seeking that is needed to construct the local covariance function. To resolve this classic "chicken - and-egg" dilemma, approximate local gravity anomalies for the Aral Sea are first predicted using Rapp's global covariance functions (shown in Figure 10) and the gridded geoid data. Based on this approximate local gravity-anomaly information, a set of empirical local covariance functions (shown in Figure 6) for the Aral Sea is derived by numerical convolution.

It should be noted that the maximum of the local empirical geoid-gravity covariance function is offset from the origin by about 0.2°. Such anomalous behavior in the correlation function and its implications for collocation will be discussed in the following section. A contour map of the collocation gravity anomalies predicted using the local empirical covariance functions is shown in Figure 12. The estimated error in the gravity prediction is about 36 mgal. The range of the predicted gravity anomalies is about -34 to 42 mgal. A contour map of the reference gravity anomalies over the Aral Sea derived from Rapp's 180 x 180 geopotential model is shown in Figure 13.

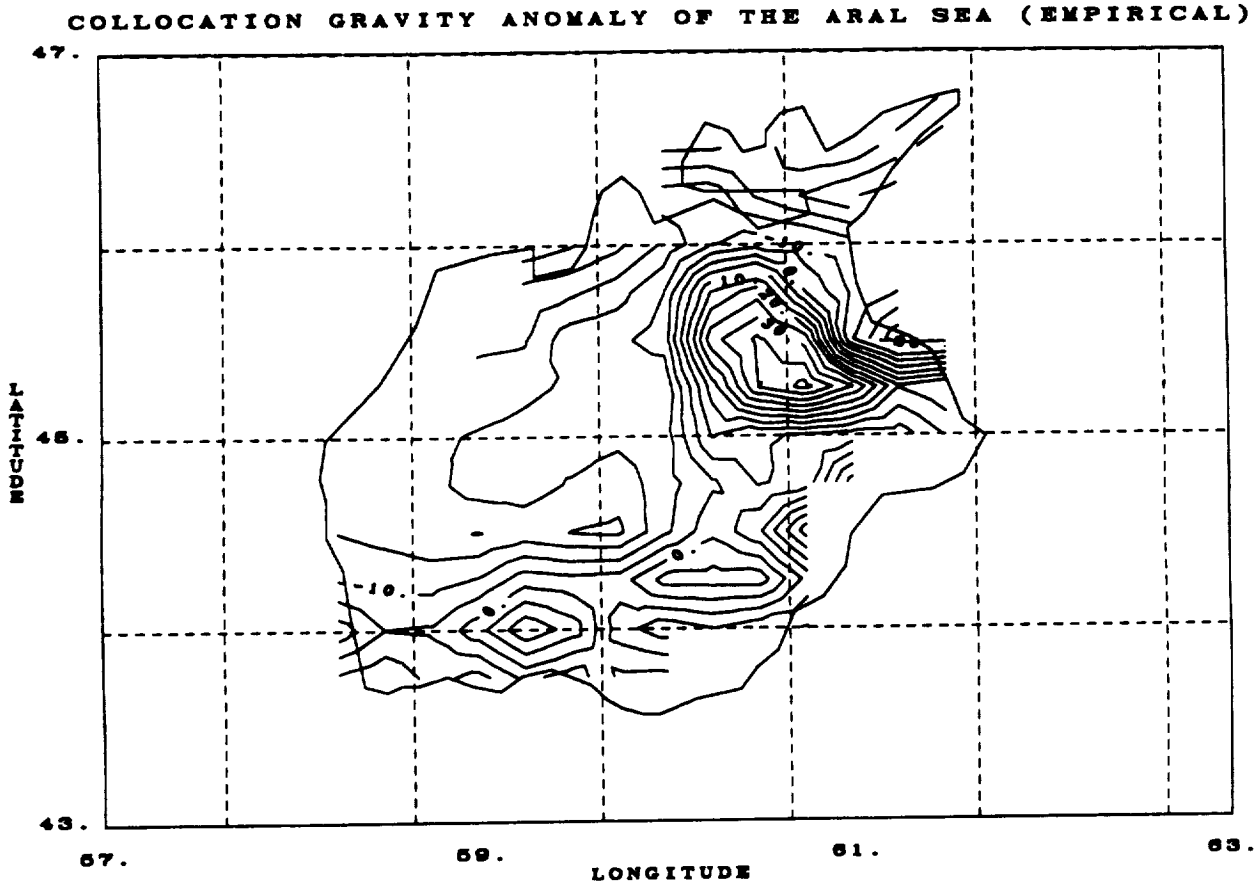

Figure 12. A contour map of estimated gravity anomalies of the Aral Sea predicted with local empirical covariance functions.

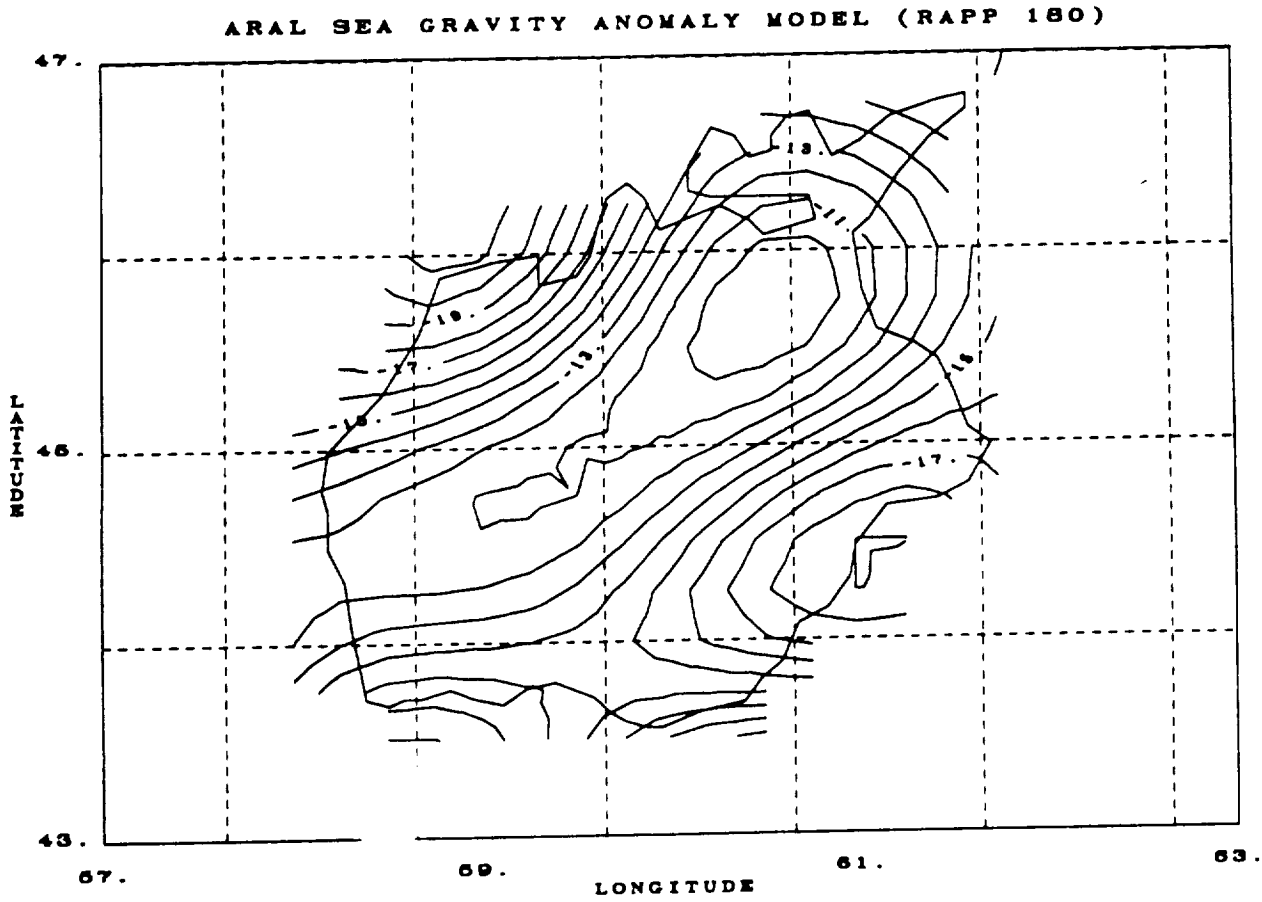

Figure 13. A contour map of Rapp's 180 x 180 reference gravity anomalies of the Aral Sea.

IV. DISCUSSION

A set of covariance functions (geoid-geoid, geoid-gravity and gravity-gravity) is a manifestation of the physical relationships (such as surface roughness and topographical phase relation) between the gravity field and the geoid undulations. In general, there is more high-frequency information in the gravity field than in the geoid undulations, because gravity is a derivative of the geoid. Thus, the half-height length of the gravity-gravity covariance functions is shorter than the geoid-geoid and geoid-gravity covariance functions. This systematic relationship is implicitly observed in Rapp's global covariance functions, and explicitly expressed in Jordan's theoretical self-consistent covariance functions. Ideally, locally derived empirical covariance functions should also reflect this systematic relationship.

However, this is not the case if local high-frequency information is not available because of a lack of surface observations. This scenario is exemplified in the set of empirical local covariance functions for the Caspian Sea (see Au *et al.*, 1989a), which are practically identical except for their covariance amplitudes. For a local region where high-frequency surface observations are not available, hybrid local covariance functions based on Jordan's formulation and using locally derived covariance parameters (covariance amplitudes and correlation length) would be the logical choice. A benchmark test of the viability of such a hybrid collocation technique has been performed (Au *et al.*, 1989a).

The peak amplitude of the local empirical geoid-gravity covariance function (see Figure 6), however, is offset from the origin by about 0.2° (a case of the split maxima), although the other two functions conform with the traditional shape. It can be argued that such anomalous behavior may be an artifact caused by the limited extent of the region involved in the convolution process. This argument fails because the origin offset is not observed in the geoid-geoid and gravity-gravity covariance functions.

In other disciplines, split maxima in correlation functions reveal underlying special symmetries in the preconvoluted functions. For example, planar twinning in crystals can be deduced from the split maxima in their crystallographic correlation function (Cowley and Au, 1978).

The split maximum in our geodetic covariance function may be related to the symmetries of the reference geoid surface and reference gravity-anomaly surface. The reference geoid surface approximates an inclined plane, whereas the reference gravity-anomaly surface is basically a saddle with the ridge running northeast to southwest. This special geometry is manifested as a split maximum in the correlation function. Such special geometry of the Aral Sea is not seen in the conventional covariance functions of Rapp, nor in Jordan's self-consistent covariance functions because the Rapp and Jordan covariance functions are derived according to models, not according to local topographic symmetries. This special geometry justifies the use of the local empirical covariance functions for both geoid gridding and gravity prediction for the Aral Sea.

To test this symmetry hypothesis, the resultant geoid undulations and gravity anomalies are used to construct a new set of local empirical covariance functions. A split maximum of the geoid-gravity covariance function persists, independent of the type of covariance functions used in the prediction. This phenomenon must, therefore, be inherent either in the altimeter data or in the process of numerical convolution.

It is observed in the altimetry analysis over the Black and Caspian Seas (Au *et al.*, 1989a) that the results of gravity prediction from geoid data are sensitive to the choice of covariance functions. Comparing the geoid results based on Rapp's global covariance function with those based on the local empirical and the hybrid Jordan's covariance functions, it is noted that geoid interpolation is rather insensitive to the choice of covariance functions, even when the covariance functions are very different. The correlation length of Rapp's covariance function is about 1.3°, whereas that of the empirical covariance functions is about 0.1°. The corresponding covariance amplitudes are 1 m for Rapp's geoid-geoid covariance function and 1.6 m for the empirical geoid-geoid covariance function.

To illustrate the dependence of the gravity prediction results on the choice of covariance functions, Jordan's self-consistent covariance functions are used in the collocation prediction of gravity anomalies over the Aral Sea. The gravity-gravity covariance amplitude is extracted from the local empirical gravity-gravity covariance function. With the previously determined geoid-geoid covariance amplitude and correlation length, a complete set of self-consistent Jordan covariance functions for the geoid-to-gravity transformation was calculated for the gravity prediction (shown in Figure 8). The contour map of the estimated gravity anomalies of the Aral Sea based on Jordan's covariance functions is shown in Figure 14. The estimated error of the predicted gravity anomalies is about 28 mgal. The range of the predicted gravity anomalies is about -75 to 254 mgal.

Gravity prediction is also performed with Rapp's global covariance functions, and the results are contoured in Figure 15. The estimated error in this gravity prediction is about 5 mgal. The range of the predicted gravity anomalies based on Rapp's covariance functions is even larger; it is about -282 to 234 mgal. Again, the estimated errors for gravity prediction reflect the difference of the gravity-gravity covariance amplitudes of the covariance functions.

To facilitate the comparison between the gravity anomalies predicted by Rapp's global covariance functions to those by the local empirical and Jordan's covariance functions, degrees of "roughness" of the gridded geoid undulations (σ^2_h) and the predicted gravity anomalies, (σ^2_g), are determined by summing the square of the residuals between the individual predicted values and their local predicted means. According to Kaula's rule, the ratio of σ_g to σ_h for a 15' grid is about 111 mgal/m based on global data. The values of σ_h for the gridded geoid based on Rapp's covariance functions, Jordan's covariance functions, and local empirical covariance functions are 28.5 cm, 30.8 cm, and 31.0 cm, respectively. The corresponding σ_g values for the three covariance functions are 747.8 mgal, 599.0 mgal and 160.6 mgal, respectively. The Kaula's ratio is then 2627 mgal/m for the geoid and gravity results obtained based on Rapp's global covariance functions, 1932 mgal/m based on the hybrid covariance functions of Jordan, and 517 mgal/m based on the local empirical covariance functions.

Judged on the basis of the Kaula's ratio, the gravity prediction using local empirical covariance functions appears to be more realistic. The gravity anomalies predicted with the local empirical covariance functions were substantially different from those predicted with the Rapp's and Jordan's covariance functions.

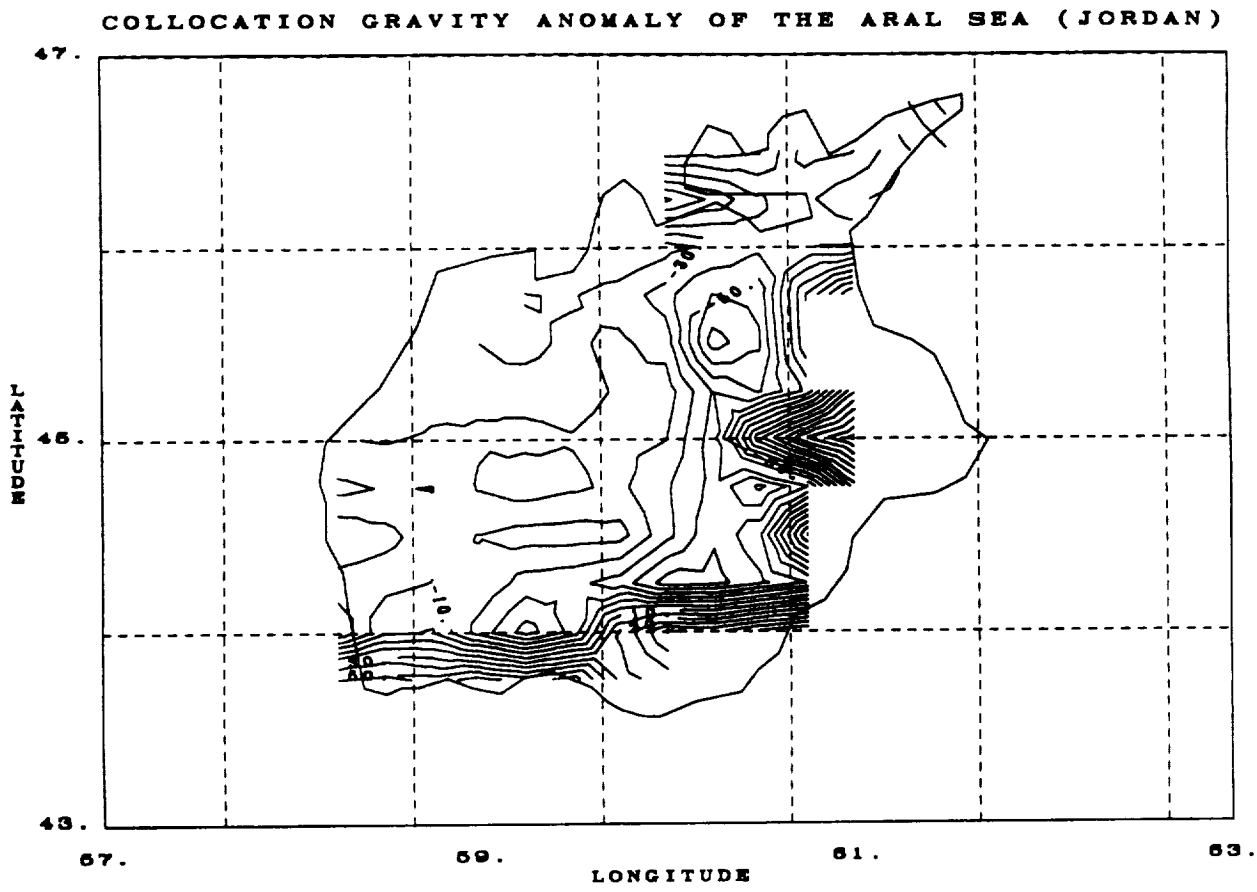

Figure 14. A contour map of estimated gravity anomalies of the Aral Sea predicted with Jordan's covariance functions.

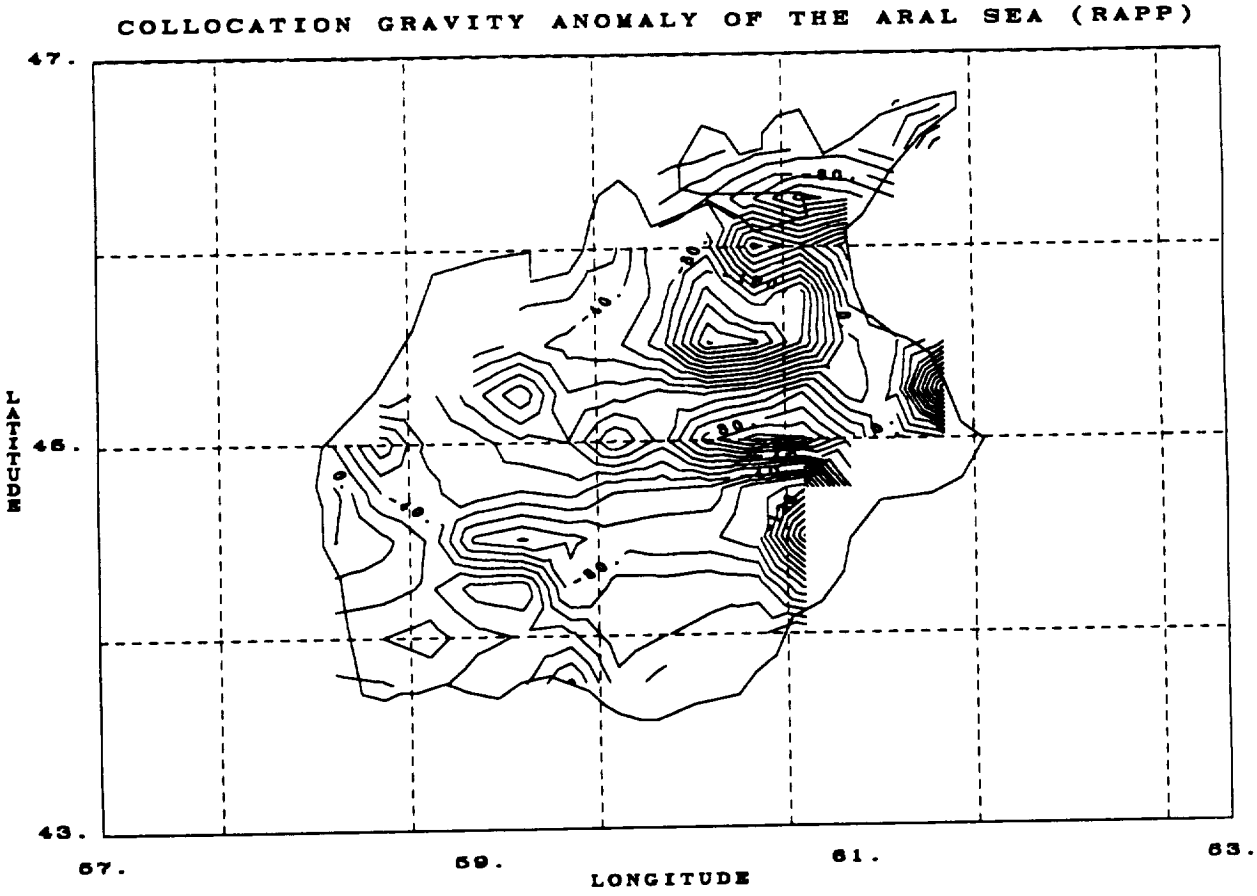

Figure 15. A contour map of estimated gravity anomalies of the Aral Sea predicted with Rapp's global covariance functions.

The gravity anomalies predicted with the local empirical covariance functions resemble the reference model, except for addition of high-frequency features. The predicted results showed a prominent gravity high at the eastern part of the sea. In contrast, according to the gravity predicted with the covariance functions of Rapp, there is a considerably low anomaly region at the northeastern part of the Aral Sea. It can be concluded that Rapp's covariance functions do not represent the phase relation between geoid undulations and gravity anomalies in the Aral Sea region.

REFERENCES

Au, A.Y., R.D. Brown, and J.E. Welker, 1989a, *Analysis of Altimetry Over Inland Seas*, NASA Technical Memorandum 100729, Washington, DC.

Au, A.Y., R.D. Brown, and J.E. Welker, 1989b, *User's Guide. Programs for Processing Altimeter Data Over Inland Seas*, NASA Technical Memorandum 100730, Washington, DC.

Cowley, J.M. and A.Y Au, 1978, "Diffraction by crystals with planar faults. III: Structure analysis using microtwins," *Acta Crystallogr.*, **B34**, pp. 739-743.

Jordan, S.K., 1972, "Self-constant statistical models for gravity anomaly, vertical deflections, and undulation of the geoid," *J. Geophys. Res.*, **77**, pp. 3660-3670.

Kaula, W.M., 1963, "The investigation of the gravitational fields of the moon and planets with artificial satellites," *Adv. in Space Sci. & Tech.*, **5**, pp. 210-226.

Knudsen, P., 1987, "Estimation and modelling of the local empirical covariance function using gravity and satellite altimeter data," *Bull. Geod.*, **61**, pp. 145-160.

Knudsen, P., 1988, *Determination of Local Empirical Covariance Functions from Residual Terrain Reduced Altimeter Data*, Reports of the Department of Geodetic Science and Surveying, **No. 395**, The Ohio State University, Columbus, OH.

Mazzega, P. and S. Houry, 1989, "An experiment to invert SEASAT altimetry for the Mediterranean and Black Sea mean surfaces," *Geophys. Jour.*, **96**, pp. 259-272.

Moritz, H., 1978, "Least-squares collocation," *Rev. Geophys. Space Phys.*, **16**, pp. 421-430.

Rapp. R.H., 1986, "Gravity anomalies and sea surface heights derived from a combined GEOS-3/SEASAT altimeter data set," *J. Geophys. Res.*, **91**, pp. 4867-4876.

Treitel, S. and E.A. Robinson, 1966, "The design of high-resolution digital filters," *IEEE Trans. on Geoscience Electronics*, **GE-4**, pp. 25-38.

NASA
National Aeronautics and Space Administration

Report Documentation Page

1. Report No.	2. Government Accession No.	3. Recipient's Catalog No.
NASA TM 100759		

4. Title and Subtitle	5. Report Date
Analysis of Altimetry Over the Aral Sea	July 1991
	6. Performing Organization Code: 921.0

7. Author(s)	8. Performing Organization Report No.
Andrew Y. Au, Richard D. Brown, and Jean E. Welker	89B00108
	10. Work Unit No.

9. Performing Organization Name and Address	11. Contract or Grant No.
Goddard Space Flight Center Greenbelt, Maryland 20771	
	13. Type of Report and Period Covered: Technical Memorandum

12. Sponsoring Agency Name and Address	14. Sponsoring Agency Code
National Aeronautics and Space Administration Washington, D.C. 20546-0001	

15. Supplementary Notes

Andrew Y. Au and Richard D. Brown: ST Systems Corporation, Lanham, Maryland;
Jean E. Welker: NASA/Goddard Space Flight Center, Greenbelt, Maryland.

16. Abstract

Satellite-based altimetric data taken by GEOS-3, Seasat and Geosat over the Aral Sea are analyzed and a least-squares collocation technique is used to predict the geoid undulations on a 0.25° x 0.25° grid and to transform these geoid undulations to free air gravity anomalies. Rapp's 180 x 180 geopotential model is taken as the reference model. The collocation procedure is performed with a set of local residual empirical covariance functions. For comparison, Rapp's global covariance functions and Jordan's self-consistent theoretical covariance functions based on Jordan's formulation and on locally derived parameters are also used to grid geoid undulations and to predict gravity anomalies. The sensitivity of the collocation results to the choice of covariance functions is discussed.

17. Key Words (Suggested by Author(s))	18. Distribution Statement
satellite altimetry, inland seas, geoid, gravitational anomalies	Unclassified - Unlimited Subject Category 46

19. Security Classif. (of this report)	20. Security Classif. (of this page)	21. No. of pages	22. Price
Unclassified	Unclassified	29	

National Aeronautics and
Space Administration

Washington, D.C.
20546

Official Business
Penalty for Private Use, $300

Postage and Fees Paid
National Aeronautics and
Space Administration
NASA-451

POSTMASTER

If Undeliverable (Section 158
Postal Manual) Do Not Return